INTERNATIONAL JOURNAL OF TECHNO-ENGINEERING
IJTE

ISSN: 2057-5688

# Experimental Demonstration of Bidirectional OFDM/OQAM-MIMO Signal Over a Multicore Fiber System

A SIVA KRISHNA YADAV [1], Dr. M NAGESWARARAO [2]

[1]Assistant professor, [2] Associate professor
Department of Electronics and Communication Engineering

ECE Department, Sri *Mittapalli College* of *Engineering*, *Guntur*, *Andhra Pradesh*-522233

***Abstract***: *A bidirectional transmission and massive multi-input multi-output (MIMO) enabled radio over a multicore fiber system with centralized optical carrier delivery is experimentally investigated in this paper. Optical carriers for upstream are delivered from the central office to the remote antenna unit via the inner core for the coreless implementation. In our experiment, as one of the fifth-generation (5G) waveform candidates, orthogonal frequency division multiplexing using offset quadrature amplitude modulation (OFDM/OQAM) is adopted in both uplink and downlink to increase the spectral efficiency and side lobes suppression ratio. An advanced 2 × 2 MIMO-OFDM/OQAM channel estimation algorithm is optimally designed to equalize the hybrid optical and wireless MIMO channels. The experimental results show that bidirectional transmission of 4.46 Gb/s 2 × 2 MIMO-OFDM/16-OQAM could be achieved over a 20-km seven-core fiber and a 0.4-m wireless link. The proposed scheme proves that the multicore fiber can realize the transparent transmission of bidirectional radio signals and effectively simplify the infrastructures in the future 5G cellular systems.*

***Index Terms***: *Orthogonal frequency division multiplexing using offset quadrature amplitude modulation (OFDM/OQAM), multicore fiber (MCF), radio over fiber (RoF), optical communication.*

## INTRODUCTION

Recently, fifth-generation (5G) mobile communication network technologies have been proposed to meet the explosive demand of mobile data capacity. It has been predicted that the 5G cellular system should be able to support 1000-fold gains in capacity and a 10 Gb/s individual user peak access rate experience [1]. To reach such high data rate, high-spectral-efficiency modulation format and massive multi-input multi-output (MIMO) technologies are indispensable. Moreover, radio over fiber (RoF) is also regarded as a considerable technique as it supports long-distance transmission and broadband wireless signals with centralized signal processing and low-cost implementation [2]. As one of the most popular modulation techniques, orthogonal frequency division multiplex (OFDM) has been widely used in Long-Term Evolution (LTE) systems [3], [4]. The requirement of cyclic prefix (CP) will limit the spectral efficiency, although it is utilized to resist inter symbol interference (ISI) and inter carrier interference (ICI). To achieve better spectral efficiency (SE), as one of the filter bank multicarrier modulation format (FBMC), OFDM using offset quadrature amplitude modulation (OFDM/OQAM) is introduced [5], [6]. In OFDM/OQAM, the used filters with good localization in time and frequency domains not only sharp a higher side lobes suppression ratio of pulse spectrum but also help to resist ISI and ICI without using CP, leading to the increase of SE [5]. The high side lobe suppression ratio makes OFDM/OQAM

ISSN: 2057-5688

more promising in narrow guard interval (GI) or carrier aggregation applications [6].

MIMO-based spatial multiplexing is another powerful technique for increasing channel capacity [7]. To deliver the signal to lots of antennas in the remote antenna units (RAUs), optical multiplexing techniques are required for low-cost implementation. Polarization division multiplexing (PDM) [8] and wavelength division multiplexing (WDM) [9] techniques are already considered in RoF systems. Moreover, optical space division multiplexing (SDM) technique based on multicore-fiber (MCF) has great potential for application in current LTE-advanced system [10], [11] and the future 5G cellular system, due to its compactness and spatial parallelism to support a lot of MIMO channels [12]. In general, the PDM technique can only provide two channels. The WDM technique is expensive due to the use of multi-wavelength laser sources. Actually, the MCF has the weakness of high cost in fiber and fan in/out devices fabrication, but the MCF also has the advantage of low inter-core crosstalk and supporting high spatial dimensions. We believe that MCF-based SDM technique has potential use in future cellular system for its high capacity of supporting massive MIMO implementation.

Recently, we have reported an experimental study on the transmission of three groups of 2 × 2 MIMO-OFDM/OQAM signals over 7-core MCF and wireless link and the impact of optical intercore crosstalk in 7-core fibers on this radio over multi-core fiber [12]. However, the MCF-based RoF schemes mentioned above only focus on downlink transmission for demonstration purpose. Although a concept of reconfigurable radio access networks using multicore fiber has already been proposed, no experimental verification has been done. Nevertheless, a more comprehensive investigation on the bidirectional RoF transmission based on multicore fiber is highly desired.

To further improve the transmission capacity and make MCF more feasible to deploy in practical 5G cellular system, in this paper, we propose a bidirectional N × N MIMO signal over 2N + 1 core fiber system. Five spatial dimensions are used to experimentally demonstrate the bidirectional 2 × 2 MIMO OFDM/OQAM radio over 20 km 7-core MCF and 0.4 m wireless link. A total of 5 cores are used in this system, where the middle core is used to deliver the seed light to RAU for coreless upstream transmission, and four rest outer cores are used for bidirectional transmission. An advanced 2 × 2 MIMO-OFDM/OQAM channel estimation algorithm is optimally designed to equalize the hybrid optical and wireless MIMO channels. The experimental results show that the multicore fiber can transparently transmit radio MIMO channels with simplest wireless front haul configuration. Besides, the multicore fiber can also support large scale of MIMO channels with optimal design of high dense core fibers.

## LITERATURE SURVEY

Fig. 1 illustrates the bidirectional N × N MIMO signal over 2N + 1 core fiber system. For the downstream transmission, at the central office (CO) N channel input signals with the same RF frequency f RF are modulated by an array of laser diode (LD). The generated optical signals are launched into N cores by the 2N + 1 core fiber fan-in device, and then be captured by an array of photodiode (PD) after M-km MCF propagation and 2N + 1 core fiber fan-out device. Subsequently, the N channel RF signals are fed into antenna array for wireless transmission. For the upstream transmission, a continuous wave (CW) laser with wavelength λup at the CO is delivered to RAU by using the middle core, and then be divided into N equal parts by a power splitter (PS). Each one is modulated by the received RF signal from antenna array at the optical modulator array. The generated N channel upstream signals are launched into the rest N cores and are then captured and recovered by

INTERNATIONAL JOURNAL OF TECHNO-ENGINEERING
IJTE
ISSN: 2057-5688

an array of PD, the analog to digital convertor (ADC), and the digital signal process (DSP) module after M-km MCF propagation. The wavelength reuse technique is used in this structure where the seed CW laser is delivered to RAU In RAU, the low-cost reflective semiconductor amplifiers (RSOA) array can be used to transmit the upstream data. Meanwhile, it should be noted that the seed light and upstream data are transmitted in different cores; thus, the Rayleigh backscattering effect from the seed light can be avoid.

Fig. 2 shows the operating principle of DFT-based N × N MIMO-OFDM/OQAM system. N channel data streams are modulated by N OFDM/OQAM modulators respectively before

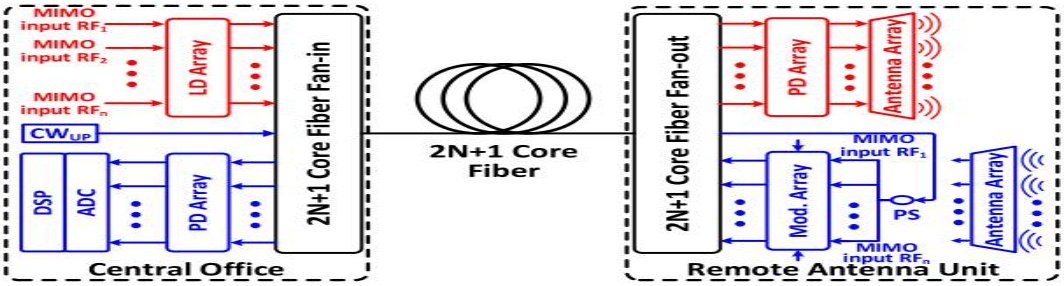


Fig. 1. Schematic of the bidirectional N × N MIMO radio over 2N + 1 core fiber system.

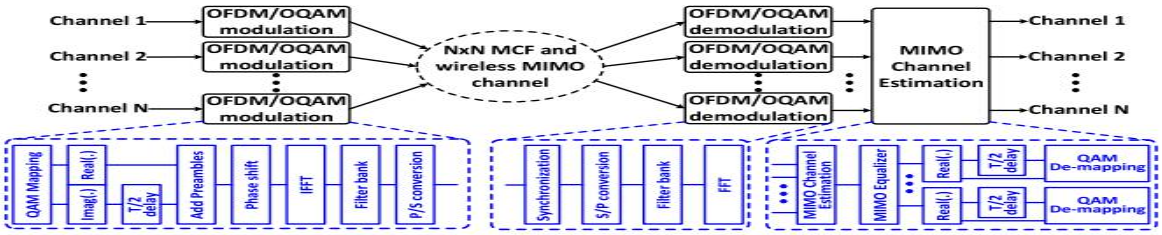


Fig. 2. Principle of DFT-based N × N MIMO-OFDM/OQAM system.

OFDM/OQAM signal, which can be expressed as

$$S(t) = \sum_{m=0}^{M-1} \sum_{n=0}^{2N-1} a_{m,n} g(t - n\tau_0) e^{j2\pi m F_0 t} e^{j\frac{\pi}{2}(m+n-2)} \quad (1)$$

After MCF and wireless transmission, N channel received signals are demodulated by N OFDM/OQAM demodulators, respectively, and then, the MIMO channel estimation module could be used to recover N channel data streams. In each OFDM/OQAM MCF and wireless transmission. In each OFDM/OQAM modulator, the input data stream is mapped into QAM format. The real and imaginary part of the generated signal are separated and the imaginary part is delayed by half symbol period. Thus, the half symbol duration τ0 and subcarrier spacing F 0 satisfy the condition τ0F 0 = 1/2. After inserting preambles for channel estimation and synchronization, the phase of each point is shifted by (m + n − 2) × π/2, where m is the index of subcarrier and n is the index of symbol. After IFFT, each symbol is filtered by a bank of FIR shaping filters. At last, a P/S converter is used to generate the baseband continuous-time

demodulator, synchronization, serial to parallel (S/P) conversion, FIR filters and FFT modules are used to transform the received signal into frequency domain. After hybrid channel estimation and MIMO equalization algorithm, the real field orthogonality in each channel could be maintained and then the obtained offset QAM signals could be transformed into QAM signals just by delaying half symbol period and combing back to the complex form again.

INTERNATIONAL JOURNAL OF TECHNO-ENGINEERING
IJTE
ISSN: 2057-5688

For the proposed bidirectional N × N MIMO RoF system, when considering the channel noises from both optical link and wireless link and taking 2 × 2 channels for example, the downlink MIMO channel model in frequency domain could be expressed as

$$\begin{bmatrix} y_1 \\ y_2 \end{bmatrix} = \begin{bmatrix} h_{11} & h_{12} \\ h_{21} & h_{22} \end{bmatrix} \left( \begin{bmatrix} H_{Fcore1} & H_{Fcore2to1} \\ H_{Fcore2to1} & H_{Fcore2} \end{bmatrix} \begin{bmatrix} x_1 \\ x_2 \end{bmatrix} + \begin{bmatrix} n_1 \\ n_2 \end{bmatrix} \right) + \begin{bmatrix} w_1 \\ w_2 \end{bmatrix} \approx \begin{bmatrix} h_{11} & h_{12} \\ h_{21} & h_{22} \end{bmatrix} \begin{bmatrix} x_1 \\ x_2 \end{bmatrix} + \begin{bmatrix} h_{11}n_1 + h_{12}n_2 + w_1 \\ h_{21}n_1 + h_{22}n_2 + w_2 \end{bmatrix} \quad (2)$$

where the matrix H F represents the MCF channel of two cores. Because the inter-core crosstalk of the used MCF is below −45 dB/100 km, the interference terms in H F could be neglected. n 1 and n 2 are the random noises in these two optical links. The matrix of h represents the wireless MIMO channel response, and w 1 and w 2 are the noises in wireless link.

Similarly, the uplink 2 × 2 MIMO channel model in frequency domain could be described as

$$\begin{bmatrix} y_1 \\ y_2 \end{bmatrix} = \begin{bmatrix} H_{Fcore1} & H_{Fcore2to1} \\ H_{Fcore2to1} & H_{Fcore2} \end{bmatrix} \left( \begin{bmatrix} h_{11} & h_{12} \\ h_{21} & h_{22} \end{bmatrix} \begin{bmatrix} x_1 \\ x_2 \end{bmatrix} + \begin{bmatrix} w_1 \\ w_2 \end{bmatrix} \right) + \begin{bmatrix} n_1 \\ n_2 \end{bmatrix} \approx \begin{bmatrix} h_{11} & h_{12} \\ h_{21} & h_{22} \end{bmatrix} \begin{bmatrix} x_1 \\ x_2 \end{bmatrix} + \begin{bmatrix} n_1 + w_1 \\ n_2 + w_2 \end{bmatrix} \quad (3)$$

where the matrix H F and the matrix of h are the MCF and wireless link MIMO channel response, respectively, and the vector of n 1,2 and w 1,2 are the random noises from optical link and wireless channel respectively. Similarly, the interference items in H F can be also ignored due to the lower inter-core crosstalk of the used MCF. Comparatively analyzing (2) and (3), it could be clearly observed that different noise distribution in optical and wireless links will lead to different

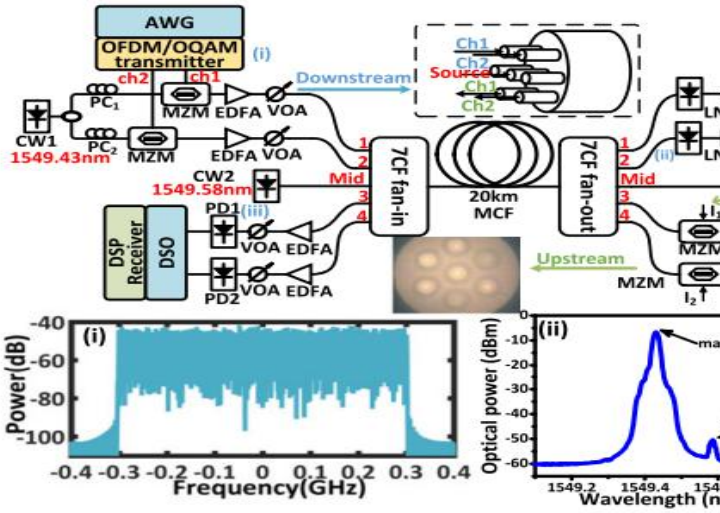


Fig. 3. Experimental setup of the proposed bidirectional N dimens
fiber.

transmission performance of uplink and downlink.

To simplify the analysis, we combine the MCF and wireless link into a hybrid channel and ignore the noises differences. The frequency domain channel model for both uplink and downlink could be expressed as

$$\begin{bmatrix} y_1 \\ y_2 \end{bmatrix} = \begin{bmatrix} hb_{11} & hb_{12} \\ hb_{21} & hb_{22} \end{bmatrix} \begin{bmatrix} x_1 \\ x_2 \end{bmatrix} + \begin{bmatrix} N_1 \\ N_2 \end{bmatrix}, \quad (4)$$

where x 1,2 and y 1,2 are the transmitted and the received signals for two channels, respectively, and N1,2 are the unified hybrid channel noises. To estimate the hybrid MIMO channel response hb, the full loaded preambles of [p , p ] T and [p , −p ] T is used in our experiment . By using the least square (LS) channel estimator and interference cancellation (IC) method, the estimated channel response can be easily calculated as

$$\begin{bmatrix} H_{11} & H_{12} \\ H_{21} & H_{22} \end{bmatrix} \approx \begin{bmatrix} y_{11} & y_{12} \\ y_{21} & y_{22} \end{bmatrix} \begin{bmatrix} p + jI_{p11} & p + jI_{p12} \\ p + jI_{p21} & -p + jI_{p22} \end{bmatrix}^{-1}, \quad (5)$$

where y 11 and y 12 stand for the received training symbols in one channel, like y 21 and y 22 for another channel. Matrix p and matrix H are the transmitted training symbols and estimated MIMO channel response, respectively, and symbol I represents the

INTERNATIONAL JOURNAL OF TECHNO-ENGINEERING
IJTE
ISSN: 2057-5688

interference calculation. Finally, we can obtain the received signals by using the estimated channel response H .

## RESULTS

The experimental setup of the proposed scheme is shown in Fig. 3. At the central office (CO), an arbitrary waveform generator (AWG, AWG7122B) with a sample rate of 10 GSa/s is used to generate two-channel RF MIMO OFDM/OQAM signals. For each channel, 192 subcarriers of 16 offset QAM and 256-point IFFT are adopted for OFDM/OQAM modulation, and noting that no CP is used here. The used pulse shaping filter is raised root cosine with roll off factor of 1, and the filter length is four times the length of one symbol. We employ eight training symbols for every 100 payload symbols, where one is for time synchronization and two are for 2 × 2 MIMO channel estimation. The two MIMO training symbols are full loaded in a manner of [A, A]T and [A, −A]T. These two generated baseband OFDM/OQAM signal are then up-converted to 2.2 GHz in the AWG. As a result, the net rate can reach to 4.42 Gb/s (2 × 10G Sa/s/12.5 × 4 × (100 − 8)/100 × 192/256) with 600 MHz bandwidth (10G Sa/s/12.5 × 192/256). A 100 kHz-linewidth continuous-wave (CW) external cavity laser (ECL, λ1 = 1549.43 nm) is used as the optical source for downstream. This optical source is firstly split into two parts by an optical coupler (OC). The two OFDM/OQAM signals are then modulated onto these two optical carriers by two Mach-Zehnder modulators (MZMs), respectively. Subsequently, these two optical signals are coupled into seven-core MCF by the self-developed fanin/fan-out devices with low loss and low crosstalk. The used seven-core MCF have a step refractive index profile and low crosstalk of −45 dB/100 km between adjacent cores is achieved. The cross section view of this MCF is shown in the inset of Fig. 3. After 20 km MCF propagation and the fan-out device, the optical signals are detected by two 10 GHz bandwidth photodiodes (PD). After two lower noise amplifiers (LNAs) with 27 dB gain, the generated RF OFDM/OQAM signals are fed into two antennas. The horizontal spacing between two Tx antennas and two Rx antennas are both 0.1 m, and the vertical spacing between Tx antennas and Rx antennas are both 0.4 m. After 0.4 m air transmission, these two wireless

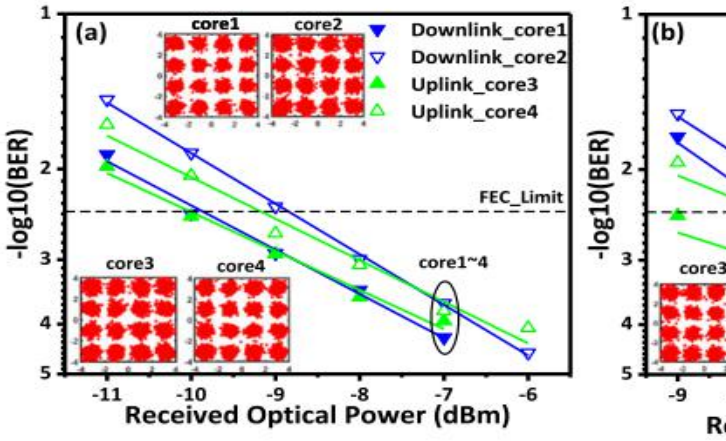


Fig. 4. BER performance of downlink and uplink in (a) without wire

signals are received by two receiver antennas and then captured by a 25 GSa/s digital sampling oscilloscope (DSO, Tektronix DPO72504DX). Offline signal processing including resampling, time synchronization, MIMO channel estimation, data mapping and BER counting is performed. A total of 7 × 105 bits are calculated for BER counting in our experiment. Inset (i) of Fig. 3 shows the electronic spectrum of the baseband OFDM/OQAM signal.

For the uplink transmission, another 100 kHz-linewidth continuous-wave (CW) external cavity laser (ECL, λ2 = 1549.586 nm) is launched into the middle core of the MCF in CO. after 20 km MCF propagation, the seed source is split into two parts by an OC. Subsequently, the received upstream wireless signal after 0.4 m air propagation are used to modulate these two CWs by two MZMs. The generated two optical signals are then coupled into the core 3 and core 4 of the MCF. After 20 km MCF propagation, the upstream signals are captured by two 10 GHz PDs and the 25 GSa/s digital sampling oscilloscope (DSO,

ISSN: 2057-5688

Tektronix DPO72504DX). The same digital signal process as used in downstream transmission is performed, and the net rat of the upstream is also 4.42 Gb/s, due to the use of the same modulation parameters.

Inset (ii) and (iii) of the Fig. 3 are the received optical spectra of the optical signals before PD in the downlink and uplink respectively, and both inter-core and Rayleigh scatter crosstalk could be clearly observed. For the downstream transmission, the optical signal in core 1 and core 2 are influenced by not only the Rayleigh scatter crosstalk from the optical signal in core 3 and core 4, but also the inter-core crosstalk from the optical signal in middle core. Therefore, the sub peak at 1549.586 nm could be clearly observed in inset (ii) of the Fig. 3. However, for the upstream transmission, the optical signal in core 3 and core 4 are only influenced by the Rayleigh scatter crosstalk from the core 1, core 2, and middle core. The negligible sub peak at 1549.43 nm in the inset (iii) of Fig. 3 illustrate that the Rayleigh scatter crosstalk is obviously lower than the inter-core crosstalk in this MCF.

Fig. 4(a) shows the measured BER performance in terms of received optical power in the PD for 2 × 2 MIMO-OFDM/OQAM with 20 km MCF and without air transmission in both uplink and downlink. It could be clearly observed that the receiver's sensitivity at the forward-error correction (FEC) limit (BER of 3.8 × 10−3) are −9.86 dBm and −8.83 dBm for two channels of the downlink respectively, and −10 dBm and −9.13 dBm for two channels of the uplink, respectively. The power penalty between each channel in both downlink and uplink could be attributed to the different performance of optical and electrical components. The insets in Fig. 4(a) are the received constellations of four cores when the received optical power at the PDs are −7 dBm.

Fig. 4(b) shows the measured BER performance for 2 × 2 MIMO-OFDM/OQAM with 20 km MCF and 0.4 m air transmission in both uplink and downlink. For downlink transmission, the receiver sensitivity for two channels at 3.8 × 10−3 FEC limit is −7.39 dBm and −6.67 dBm, respectively.

Compared to Fig. 4(a), about 2.5 dB power penalty is observed when the wireless link is added. This could be attributed to the decreased signal to noise ratio (SNR) in the air transmission. For uplink transmission, the receiver sensitivity for two channels at 3.8 × 10−3 FEC limit is −9.01 dBm and −7.56 dBm respectively. Similarly, about 1.2 dB power penalty is observed due to the decreased SNR. Different power penalty in uplink and downlink could be explained by the different position of wireless link. In downstream transmission, each MIMO signal is launched into MCF and then into air transmission link. However, in upstream transmission, each MIMO signal is launched into air link and then into MCF. Noting that the crosstalk between antennas is larger than inter-core crosstalk in MCF. As mentioned in Section 2, the different channel noise items will have different influence to the used LS MIMO equalization algorithm. Besides, the different optical and electronic components in uplink and downlink will also change the trends of BER curves. The insets in Fig. 3(b) are the received constellations at the received power of −4 dBm for both downlink and uplink, respectively. It should be noted that only two 2 × 2 MIMO is investigated in our experiment due to the limitation of the channel numbers of the used AWG. However, the 2 × 2 MIMO channel estimation algorithm could be easily extended to N × N MIMO channel estimation algorithm when more than two input signal are transmitted. Moreover, our group has designed 64-core trench-assisted multicore fiber with maximum crosstalk less than −14 dB/20 km, by utilizing the heterogeneous core with the trench-assisted index profile. Therefore, we believe that the proposed scheme has potential

application in future 5G cellular systems with a higher density or radio-access points.

## CONCLUSION

We have experimentally demonstrated a bidirectional transmission and massive MIMO enabled radio over seven-core fiber system with centralized optical carrier delivery. In our experiment, the middle core is used to deliver the seed light to ONU for coreless upstream transmission. By using spectral efficiency OFDM/OQAM modulation technique and hybrid optical and the wireless MIMO channel estimation algorithm, bidirectional transmission of a 4.42 Gb/s 2 × 2 MIMO-OFDM/OQAM signal over a 20 km seven-core fiber and a 0.4 m wireless link are successfully achieved. These results show that the multicore fiber could satisfy the transparently transmission of bidirectional RF MIMO signals. Moreover, by using higher core density MCF, this architecture could be easily extended to support massive MIMO ROF transmission in future 5G cellular communication.

## REFERENCES

[1]. G. Jagga Rao, Y. Chalapathi Rao " Robust Bit Error Rate Optimization for MASSIVE MIMOCEM System using Channel Coding Method "in Volume 8-Issue 4S2, pp. 180-184, March 2019.

[2]. M Sumalatha,Dr. P V Naganjaneyulu, and K Satya Prasad —Low-Power and Area-Efficient FIR Filter Implementation Using CSLA with BEC‖ Journal of Microelectronics, Electromagnetics and Telecommunications,https://doi.org/10.1007/978-981-10-7329-8_14 Jan-2018,Volume -8 , Issue -3 ,ISSN: 0976-4860,pages:137-142, Springer.

[3]. A. Ravi,Dr. P. V. Naganjaneyulu ,Dr.M.N. Giriprasad —SAR images denoising using a novel stochastic diffusion wavelet scheme‖,Springer, Cluster Computing Journal ,USA,July-2017,DOI 10.1007/s10586-017-1001-6,ISSN:1573-7543,Pages:01-09,Springer.

[4]. P SekharBabu,Dr. P V Naganjaneyulu, and K Satya Prasad —Adaptive Beam Forming of MIMO System using Low Complex Selection of Steering Vector‖ International Journal of Advancements in Technology,Jan-2017,Volume -8 , Issue -3 ,ISSN: 0976-4860,pages:01-06, Elsevier.

[5]. D. Rajendra Prasad, Dr. P. V. Naganjaneyulu ,Dr. K. Satya Prasad —A Hybrid Swarm Optimization for Energy Efficient Clustering in Multi-hop Wireless Sensor Network‖ Wireless PersCommun DOI 10.1007/s11277-016-3562-8 Springer Science+Business Media New York 2016, Pages:2459-2471.

[6]. P. Ravikumar, P.V. Naganjaneyulu, K. Satya Prasad —Peak to Average Power Ratio reduction method for Orthogonal Frequency Division Multiplexing in 4G Communication‖, I J C T A, 8(5), 2015, pp. 1703-1708m.

[7]. M Sumalatha, Dr.P .V .NaganjaneyuluandDr.K .Satya Prasad —ADVANCED FAST FOURIER TRANSFORM USING RADIX-8 BOOTH MULTIPLIER‖ ISSN 2319 - 2518 Int. J. Elec&Electr.Eng& Telecoms. 2015, Special Issue, Vol. 1, No. 3,pp (27-32) November 2015.( Impact factor – 0.454 ).

[8]. U.Sreenivasulu, Dr. P.V.Naganjaneyulu, —Performance of bit-

ISSN: 2057-5688

interleaved coded multiantenna OFDMA systems over space-frequency‖ National Conference on Advanced Communication Systems &Applications,held at Madanapalli 0n June 2013 , INDIA proceedings pp.161-168.

[9]. T.Srinivas,Dr.P.V.Naganjaneyulu,P.SandeepMohan,R.Shiva Shankar ,Ch.Surender Reddy ―Face Recognition Using PCA and Bit-Plane Slicing‖ PEIE 2012, LNEE, Springer-Verlag Berlin Heidelberg 2012 , pages: 401-407, 2012.

[10]. G. Jagga Rao, Y. Chalapathi Rao, Dr. Anupama Desh Pande "Detection For 6G-NOMA Based Machine Learning Optimization for Successive Adaptive Matching Pursuit Analysis", Q3, pp. 1803-1812, Jan 2020.

[11]. P.V. Naganjaneyulu, Dr.K.Satya Prasad, An adaptive blind channel estimation for OFDM system multimedia by improved H∞ approach (for high data rate)‖, International conference on computer intelligence and multimedia applications held at Siva Kasi on Dec. 2008, vol.4, pages:252-256, Dec. 2008, Published also in IEEE computer society in the portal.acm.in.

[12]. P.V. Naganjaneyulu, Dr.K.Satya Prasad, ―An adaptive blind channel estimation for OFDM system by improved H∞ approach‖, International Conferences on advanced communication systems held at CIT Coimbatore on Oct. 2007, preceding pages:33-36.

[13]. Dr. k. Raju, A. Sampath Dakshina Murthy, Dr. B. Chinna Rao,G. Jagga Rao "A Robust and Accurate Video Watermarking System Based On SVD Hybridation For Performance Assessment" International Journal of Engineering Trends and Technology (IJETT) – Volume 68 Issue 7 - July 2020.

[14]. P.V. Naganjaneyulu, Dr.K.Satya Prasad, ―A Study of blind channel estimation in OFDM system by H∞ approach‖, National conference on Communication and signal processing held at IEEE, Mumbai on Feb 2007, NCCSP-07, pages:20-24, Feb. 2007.

[15] J. G. Andrews et al., “What will 5G be?” IEEE J. Sel. Areas Commun., vol. 32, no. 6, pp. 1065–1082, Jun. 2014.

[16] S. E. Alavi, M. R. K. Soltanian, I. S. Amiri, M. Khalily, A. S. M. Supa’at, and H. Ahmad, “Towards 5G: a photonic based millimeter wave signal generation for applying in 5G access fronthaul,” Sci. Rep., vol. 6, no. 19891, pp. 1–11, Jan. 2016.

[17] M. Morant, J. Prat, and R. Llorente, “Radio-over-fiber optical polarization-multiplexed networks for 3GPP wireless carrier-aggregated MIMO provision,” J. Lightw. Technol., vol. 32, no. 20, pp. 3721–3727, Oct. 2014.

[18] T. Kanesan, S. Rajbhandari, E. Giacomidis, and I. Aldaya, “Nonlinear limit of alternative method to 2 × 2 MIMO for LTE RoF system,” Electron. Lett., vol. 50, no. 4, pp. 300–301, Feb. 2014.

[19] C. Li et al., “Experimental demonstration of 429.96-Gb/s OFDM/OQAM-64QAM over 400-km SSMF transmission within a 50-GHz grid,” IEEE Photon. J., vol. 6, no. 4, pp. 1–8, Aug. 2014.

[20] M. Xu, J. Zhang, F. Lu, Y. Wang, D. Guidotti, and G. K. Chang, “Investigation of FBMC in mobile fronthaul networks for 5G

ISSN: 2057-5688

wireless with time-frequency modulation adaptation," in Proc. Opt. Fiber Commun. Conf. (Opt. Soc. Amer.), 2016, Paper W3C.2.